Nanoscale

Accepted Manuscript

This article can be cited before page numbers have been issued, to do this please use: S. Jeon, C. Choi, J. Ju, S. Lee, J. H. Park and J. Kim, *Nanoscale*, 2019, DOI: 10.1039/C9NR00643E.

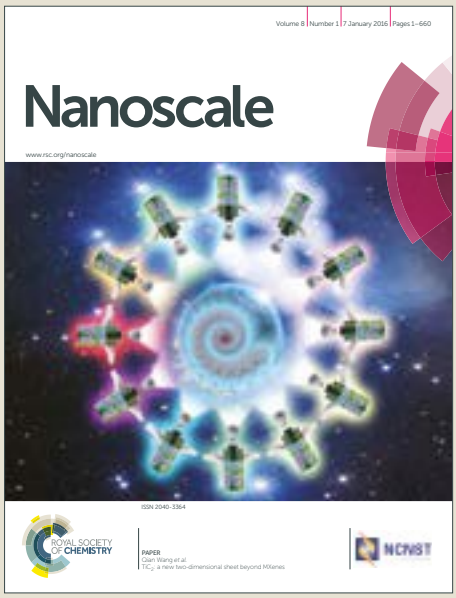

ROYAL SOCIETY OF CHEMISTRY

rsc.li/nanoscale

View Article Online
DOI: 10.1039/C9NR00643E

Tuning the Response Selectivity of Graphene Oxide Fluorescence by Organometallic Complexation for Neurotransmitter Detection

*Su-Ji Jeon, Chanhee Choi, Jong-Min Ju, Sin Lee, Jung-Hyun Park, and Jong-Ho Kim**

Department of Chemical Engineering, Hanyang University, Ansan 426-791, Republic of Korea

* To whom correspondence should be addressed: kjh75@hanyang.ac.kr

Abstract

It is of great interest to design nanomaterial biosensors that can selectively detect target molecules without the use of fragile and expensive antibodies. Here, we report a chemical approach to modulate the response selectivity of graphene oxide (GO) fluorescence for neurotransmitters, in order to design an optical biosensor for the selective detection of dopamine without using antibodies. To this end, GO was functionalized with six different amino acids, followed by the immobilization of seven metal ions, resulting in the production of forty-two different GO nanohybrids (denoted GO-AA-MI derivatives). The fluorescence response of GO-AA-MI derivatives to dopamine, norepinephrine, and epinephrine was modulated by varying the type of amino acids and metal ions introduced. Tyrosine-modified GO with Fe^{2+} ions (GO-Y-Fe) exhibited the selective quenching of its fluorescence in the presence of dopamine whereas lysine-modified GO with Au^{3+} ions (GO-K-Au) showed a selective increase in fluorescence upon addition of norepinephrine. The GO-Y-Fe sensor developed was able to differentiate dopamine from similar structures of norepinephrine and epinephrine, as well as abundant interferences such

View Article Online
DOI: 10.1039/C9NR00643E

as ascorbic acid and uric acid, without the use of antibodies. In addition, the GO-Y-Fe sensor successfully detected dopamine secreted from living neuron cells in a rapid and simple manner.

Introduction

Biosensors are of great interest in the fields of clinical diagnosis, health monitoring, fundamental biology, environmental and food analysis, and drug screening.[1-3] Various types of biosensor have been developed to date, and their sensitivity for the detection of target molecules has been improved by combining them with nanomaterials. In addition to sensitivity, the selective recognition of target molecules is a vital requirement for the design of biosensors, which is often accomplished by introducing natural antibodies to the sensor materials. Antibodies, however, are very expensive and susceptible to perturbation in both external and internal conditions; although they are still considered to be a gold standard recognition element with a high binding affinity for the target molecule of interest.[4-7] In addition, antibody-based immunoassays commonly require multistep procedures, including the use of both primary and secondary antibodies, and labeling the antibodies with fluorescent dyes or enzymes for signal transduction. These issues have driven the development of antibody-free assays,[8-12] or alternatives such as artificial antibodies[13-17] and aptamers[18-21] for the selective detection of target molecules.

Dopamine, a chemical compound with a catechol moiety, is an important neurotransmitter in the central and peripheral nervous systems and the cardiovascular systems of the human body.[22, 23] Altered dopamine levels in the human body have been associated with neural and brain disorders; causing severe neural diseases such as Parkinson's disease, schizophrenia, and dementia.[24] Hence, many efforts have been made to develop methods,

View Article Online
DOI: 10.1039/C9NR00643E

including high-performance liquid chromatography (HPLC),[25] fluorescence sensing,[11, 26-29] electrochemical measurement,[30-32] colorimetric detection,[33] and immunoassays,[34] for the selective and sensitive detection of dopamine in biological fluids. A few approaches for the antibody-free detection of dopamine have been reported,[16, 35, 36] however, it remains a challenge to develop biosensors that are able to differentiate dopamine from other catecholamines such as epinephrine and norepinephrine without the use of antibodies.

Graphene oxide (GO) is a two-dimensional carbon nanosheet with oxygen-containing functional groups obtained by the exfoliation of oxidized graphite.[37] The hydrophilic functional groups give GO excellent water dispersibility and the confined conjugated sp^2 domains for fluorescence emission.[38-43] These functional groups of GO have facilitated diverse biological applications, from biosensing to drug screening.[44-50] GO fluorescence has been employed as a signal transduction tool in biosensing because it is more resistant to photobleaching than conventional fluorophores.[51] In GO-based biosensors, the response of GO fluorescence to target molecules can be tuned by introducing recognition elements on to the surface of GO.[28, 52-55] These optical properties make GO an excellent fluorophore for designing optical biosensors for the selective detection of target molecules. In particular, it would be interesting to use simple chemical functionalization to tune the response selectivity of GO fluorescence to a specific target for antibody-free sensing.

Here, we have demonstrated a chemical approach, based on functionalization of GO with various amino acids and metal ions, for modulating the response selectivity of GO fluorescence to catecholamine neurotransmitters. This allowed the antibody-free selective detection of dopamine from other catecholamines and interferences. A variety of amino acid (AA) and metal ion (MI)-functionalized GO (GO-AA-MI) derivatives were prepared, and their fluorescence

View Article Online
DOI: 10.1039/C9NR00643E

response to dopamine, epinephrine, and norepinephrine was explored extensively. In addition, a mechanistic study of the selective response of GO fluorescence was carried out, as well as the in-vitro detection of dopamine using the selected GO-AA-MI sensor.

Experimental

1. Materials

Graphite flake, sodium nitrate ($NaNO_3$), potassium permanganate ($KMnO_4$), chloroacetic acid, sodium hydroxide (NaOH), 1-ethyl-3-(3-dimethylaminopropyl)-carbodiimide (EDC), *N*-hydroxysuccinimide (NHS), Cobalt(II) sulfate heptahydrate, Copper(II) sulfate pentahydrate, Nickel(II) sulfate hexahydrate, and zinc sulfate heptahydrate(II) were purchased from Sigma-Aldrich (St. Louis, MO, USA), and they were used without purification. Hydrochloric acid (HCl), hydrogen peroxide (H_2O_2), and sulfuric acid (H_2SO_4) were purchased from Dae-Jung Chemicals (Busan, Korea). Trifluoroacetic acid (TFA) was bought from TCI (Tokyo, JAPAN). H-Tyr(tBu)-OtBu·HCl, H-Met-OtBu · HCl, H-Ser(tBu)-OtBu, H-Lys(Boc)-OtBu · HCl, H-Trp(Boc)-OH, and H-Asp(OtBu)-OH were purchased from BACHEM (Bubendorf, Switzerland). PC-12 cells were purchased from Korean Cell Line Bank (Seoul, Korea). Roswell Park Memorial Institute (RPMI) 1640 media containing L-glutamine, HEPES, $NaHCO_3$, 50 μg ml^{-1} streptomycin, penicillin, heat inactivated fetal bovine serum (FBS), and trypsin-EDTA were purchased from Gibco® (Carlsbad, CA, USA).

2. Instruments

The ultraviolet/visible (UV/Vis) absorption of GO, GO-AA, and GO-AA-MI was measured by a UV/Vis spectrometer (UV-2600, Shimadzu, Japan). The morphology and size of

View Article Online
DOI: 10.1039/C9NR00643E

GO were characterized by an atomic force microscope (AFM, XE-100, Park systems, Korea). Elemental analysis (EA) was carried out by an elemental analyzer (CHNS-932, LECO Inc. USA). The FT-IR and XPS spectra for GO, GO-AA, and GO-AA-MI derivatives were taken by an attenuated total reflectance spectrometer (ATR, Nicolet, Thermo Scientific Inc.) and a surface analysis spectrometer (AXIS Nova, Kratos Analytical, UK), respectively. The Raman spectra of GO and GO-AA were measured by a Raman microscope (UniRAM, Uninanotech, Korea). The photoluminescence spectra were obtained by a spectrofluorometer (Nano Log®, Horiba Scientific, Tokyo, Japan). ELISA was measured by a microplate reader (MQX 200, BioTek Instruments, Winooski, VT, USA).

3. Preparation of GO

Graphite flake (0.5 g) and $NaNO_3$ (0.375 g) were slowly added to 17 ml of H_2SO_4 in an ice bath. Then, $KMnO_4$ (2.5 g) was slowly added to the graphite flake mixture in an ice bath. After stirring the resulting solution for 10 min, the temperature increased to 35 °C, and then the mixture was vigorously stirred for 2 h. After DI water (30 ml) was slowly added to the reaction mixture in an ice bath, the resulting mixture was stirred for 2 h at room temperature. Then, H_2O_2 (2 ml) was slowly added to the reaction mixture in an ice bath with vigorous stirring at room temperature until the gas was not generated. Then, the mixture was washed with a HCl aqueous solution (10 vol%, 250 ml) and DI water (1250 ml). After neutralizing the mixture solution with a 0.1 M NaOH solution, the obtained graphite oxide was washed with DI water via dialysis for 2 days. The graphite oxide solution was then sonicated for 90 min at 12 W in an ice bath. The resulting graphene oxide solution was finally centrifuged at 13,000 rpm for 1 h, and the supernatant was collected for further experiments.

View Article Online
DOI: 10.1039/C9NR00643E

4. Synthesis of GO-AA-MI derivatives

A 15 ml portion of GO aqueous solution (0.7 mg/ml) was mixed with 15 ml of DMSO, followed by the addition of 1-ethyl-3-(3-dimethylaminopropyl)-carbodiimide (EDC, 124 μmol), *N*-hydroxysuccinimide (NHS, 124 μmol), and an amino acid with t-butyl ester (124 μmol). The resulting mixture was stirred for 15 h at 25°C. Then, 30 mL of trifluoroacetic acid was added to the GO solution, and the resulting solution was stirred for 1 h at 25°C. The desired GO-AA product was purified by dialysis using a membrane (MWCO 6,000) for 48 h.

5. General procedure for the measurement of GO-AA-MI fluorescence response

To measure GO-AA fluorescence change with different metal ions, 20 μl of each metal ion solution was added to 400 μl of the GO-AA solution (0.5 μg/ml, PBS, pH 7.4). The concentration of the metal ion in the GO-AA solution varied between 10 and 100 μM. The resulting mixture was gently shaken for 10 min at 25°C. The fluorescence of GO-AA was measured under 450 nm excitation with an exposure time of 0.1 s.

In order to measure the fluorescence change of GO-AA-MI derivatives upon addition of neurotransmitters, 20 μl of each neurotransmitter solution (125 μM) was added to 400 μl of the GO-AA-MI solution (50 μg/ml, in PBS, pH 7.4). The resulting mixture was gently stirred for 15 min at 25°C, and the fluorescence of the GO-AA-MI was measured under 450 nm excitation with an exposure time of 0.1 s.

6. Determination of the quenching rate constants (k_q) of GO-AA for metal ions

View Article Online
DOI: 10.1039/C9NR00643E

The quenching rate constants (k_q) between the metal ions and GO were calculated based on the fluorescence response of GO-AA to metal ions at various concentrations using the Stern-Volmer equation;

$$I_0 / I = K_{sv} [Q] + 1, k_q = K_{sv} / \tau_0$$

, where I_0 and I are the fluorescence intensity of GO-AA in the absence and presence of a metal ion, respectively, [Q] is the concentration of a metal ion, K_{sv} is a Stern-Volmer quenching constant, $K_{sv} = k_q\tau_0$ in which k_q is a quenching rate constant and τ_0 is the lifetime of GO-AA fluorescence (0.21 ns).

7. Measurement of the cytotoxicity of GO-AA-MI using CCK assay

A 100 μl portion of cell suspension was dispensed in a 96-well plate, and then the cell suspension was incubated for 24 h in an incubator. A 10 μl portion of GO, GO-Y, or GO-Y-Fe at various concentrations was added to the cells, followed by incubation for 24 h. After a 10 μl portion of CCK-8 solution was then added to each well of the cell plate, the cells were incubated for 2 h. Finally, the absorbance at 450 nm was measured using a microplate reader.

8. Detection of dopamine secreted from PC-12 cells with GO-AA-MI

PC-12 cells were cultured in a 6 well-plate using a RPMI media containing 10% FBS and 50 UmL^{-1} penicillin at 37°C under 5% CO_2 atmosphere. A 100 μl portion of cell media was collected at each time interval, and added to 100 μl of the GO-Y-Fe solution (50 μg/ml of GO-Y-Fe). The resulting solution was stirred for 15 min at 25°C, and the fluorescence of GO-Y-Fe was measured under 450 nm excitation with an exposure time of 0.1 s.

View Article Online
DOI: 10.1039/C9NR00643E

Results and discussion

1. Preparation of GO-AA-MI derivatives

To prepare GO-AA-MI derivatives, six different amino acids (whose carboxylic acid was protected by a t-butyl ester), including aspartic acid (D), lysine (K), methionine (M), serine (S), tryptophan (W), and tyrosine (Y), were coupled to the carboxylic acid of GO (Figure 1a and Figure S1). After deprotection of the t-butyl group on the amino acid-coupled GO (GO-AA), seven types of metal ions were immobilized to produce forty-two different GO-AA-MI derivatives, each with a different combination of amino acid and metal ion. The functionalization of GO with amino acids could alter its binding affinity for metal ions, while the immobilized metal ion could change its redox reactivity.[9]

The physical structures of GO-AA-MI derivatives were first characterized using microscopic methods. The morphology and size of the GO-AA-MI derivatives remained similar with pristine GO regardless of the type of amino acid and metal ion introduced, as shown in atomic force microscopy (AFM) and transmission electron microscopy (TEM) images (Figure 1b-1e). The GO-AA-MI derivatives had an average lateral size of 150 nm with an average height of 1 nm.

The chemical structure of GO-AA-MI derivatives was analyzed by various spectroscopic methods. As shown in the Fourier transform infrared (FT-IR) spectrum of the aspartic acid-coupled GO (GO-D) (Figure 1f), the characteristic vibrational modes for amide I (C=O, 1664 cm^{-1}) and amide II (C-N-H, 1576 cm^{-1}) were clearly observed. After coupling other amino acids to the carboxylic acid of pristine GO, these amide I and II vibrational modes also appeared in the corresponding FT-IR spectra (Figure S2), indicating that the amino acids were covalently introduced to GO. The amount of each amino acid coupled to GO was quantified using elemental

View Article Online
DOI: 10.1039/C9NR00643E

analysis. The amino acids were introduced to the loading levels on the basis of their nitrogen contents, from 0.46 to 0.79 mmol/g (Table S1). The immobilization of metal ions to six different GO-AA structures was confirmed by FT-IR spectroscopy. After the introduction of cobalt ions to GO-D (denoted "GO-D-Co"), the amide I mode of GO-D-Co shifted toward a lower frequency (1651 cm^{-1}) while the C−O stretching mode of the amino acid carboxylate moiety shifted toward a higher frequency (1228 cm^{-1}) compared with GO-D (Figure 1f).[56, 57] The immobilization of the metal ions to GO-AA was confirmed in other GO-AA-MI structures using X-ray photoelectron spectroscopy (XPS). As shown in Figure 1g, the bonding energy of the amide N increased from 399 to 400 eV after immobilization of Fe^{2+} ions on tryptophan-modified GO (GO-W). Additionally, the characteristic peaks for Fe^{2+} ions were clearly observed at 711.5 and 725.6 eV in the XPS spectrum of the GO-W-Fe structure. The immobilization of the other metal ions on the GO-AA structures were also clearly observed in their XPS spectra (Figure S3). These results show that the metal ions were successfully immobilized on GO-AA, leading to the formation of various GO-AA-MI derivatives.

2. Optical properties of GO-AA-MI derivatives

The optical properties of GO-AA-MI derivatives were then investigated. After coupling amino acids to pristine GO, the electronic transition from the nonbonding orbital to the pi antibonding orbital at 300 nm increased in the absorption spectra of GO-AA structures (Figure S4a). The fluorescence of the GO-AA derivatives, however, diminished when compared to pristine GO (Figure S4b), which could be explained by the formation of more defects on the sp^2 clusters during acid treatment when deprotecting the t-butyl group from the amino acids (Figure S5 and Table S2). The chelation of seven metal ions to the GO-AA structures did not significantly influence their absorption (Figure S6), whereas it caused unique fluorescence

View Article Online
DOI: 10.1039/C9NR00643E

quenching. As shown in Figure 2a, the fluorescence of GO-D was most significantly quenched by Cu^{2+} ions, and the quenching extent gradually decreased as Fe^{2+} and Zn^{2+} ions were respectively added. This shows that the quenching extent of the GO-AA structure depends on the types of metal ion, and in particular their reduction potential (Figure 2b). The Cu^{2+} ions with a positive reduction potential are more likely to accept the excited electrons of the GO-AA than Fe^{2+} and Zn^{2+} ions with negative reduction potentials.[58] Additionally, the type of amino acid coupled to the GO was found to modulate the quenching response of GO-AA structures (Figure 2c). For instance, as Fe^{2+} ions were added, the fluorescence quenching extent of the GO-AA structures was changed by varying the amino acid. The fluorescence of GO-M was quenched from its original intensity by 40% upon addition of Fe^{2+} ions, while GO-K and GO-Y were quenched by 25% and 34%, respectively. In the case of the strongest quencher, Cu^{2+} or the weakest quencher, Zn^{2+}, the dependency of the fluorescence response of the GO-AA on the amino acid was reduced. In addition to the reduction potentials of metal ions, their binding affinity to GO-AA can also influence its fluorescence quenching. Although the reduction potential of Ag^{+} ions is more positive than that of Cu^{2+} ions, the binding affinity of Ag^{+} to the amino acids of GO-AA is much lower than that of Cu^{2+},[59] leading to a weaker fluorescence quenching in the GO-AA structures. The quenching rate constants for the metal ions clearly revealed that the fluorescence response of GO-AA structures could be modulated by varying the coupled amino acids (Table S3).

3. Fluorescence response of GO-AA-MI derivatives to neurotransmitters

Next, the fluorescence response of the forty-two GO-AA-MI derivatives to three different catecholamine neurotransmitters (dopamine, norepinephrine, and epinephrine) was measured in phosphate buffered saline (PBS, pH 7.4). As shown in Figure S7, the fluorescence changes of the

View Article Online
DOI: 10.1039/C9NR00643E

GO-AA-MI derivatives upon addition of each neurotransmitter were affected by the coupled amino acid as well as the immobilized metal ions. In the case of methionine-coupled GO with Cu^{2+} (GO-M-Cu), its fluorescence was clearly quenched by dopamine while it was hardly changed in the presence of norepinephrine or epinephrine (Figure 3a). However, when Cu^{2+} ions were immobilized on pristine GO (GO-Cu) without methionine, the selective fluorescence response to dopamine disappeared; the fluorescence quenching extent for dopamine and norepinephrine was almost identical. The effect of the coupled amino acids on fluorescence response to a target was also clearly observed in GO-AA-Au derivatives for norepinephrine (Figure S7). The fluorescence of GO-W-Au increased by 40% from its original intensity upon addition of norepinephrine whereas GO-M-Au showed a negligible increase in fluorescence. These results suggest that the functionalization of GO with various amino acids can induce a selective fluorescence response in the resulting GO-AA-MI to a target molecule.

The fluorescence response of GO-AA-MI derivatives to neurotransmitters was also modulated by the metal ions incorporated. When Cu^{2+}, Ag^{+}, or Au^{3+} ions were immobilized on lysine-coupled GO (GO-K), the corresponding GO nanohybrids (GO-K-Cu, GO-K-Ag, and GO-K-Au) showed unique fluorescence responses to each catecholamine neurotransmitter (Figure 3b). GO-K-Au exhibited a selective fluorescence increase to norepinephrine, whereas GO-K-Ag showed a selective fluorescence quenching response to epinephrine. GO-K-Cu displayed no selective fluorescence response to any of the neurotransmitters. The effect of metal ions on the fluorescence response of GO-AA-MI derivatives to a target was also observed in tyrosine-coupled GO (GO-Y) bearing each of the metal ions (GO-Y-MI) in the presence of dopamine (Figure S7). The fluorescence of GO-Y-Fe was quenched by 20% from its original intensity upon addition of dopamine, but GO-Y-Cu, GO-Y-Ni, and GO-Y-Co only showed slight

View Article Online
DOI: 10.1039/C9NR00643E

quenching responses (5%). GO-Y-Au exhibited no fluorescence quenching in the presence of dopamine. These results demonstrate that the selectivity and sensitivity of the fluorescence response of GO-AA-MI derivatives to target neurotransmitters can be modulated by varying the immobilized metal ions. Based on a comprehensive screening of the fluorescence response of different GO-AA-MI derivatives to neurotransmitters, the GO-Y-Fe and GO-M-Cu nanohybrids were found to selectively detect dopamine rather than norepinephrine and epinephrine (Figure 3c).

To elucidate the fluorescence response of GO-AA-MI derivatives to dopamine, the binding affinities of amino acids with metal ions reported in the literature[59] were plotted with the quenching response of five GO-M-MI derivatives to dopamine (Figure 4a). As the binding affinity of the amino acid methionine to metal ions increased, the quenching extent of GO-M-MI also increased. In the case of GO-D-MI derivatives, the same pattern of quenching by dopamine was observed (Figure 4b). The higher the binding affinity of aspartic acid to the metal ion, the more fluorescence quenching was observed. The oxidation of dopamine was accelerated by GO-M-Cu and GO-M-Fe as compared to GO-M without metal ions (Figure 4c); in particular, dopamine oxidation was promoted more by GO-M-Fe than GO-M-Cu (Figure S8), leading to greater fluorescence quenching in GO-M-Fe. Based on these results, a plausible mechanism for the fluorescence response of GO-AA-MI to dopamine can be proposed (Figure 4d). It is known that catechol groups bind to various metal ions[60]; therefore, dopamine could take a metal ion from GO-M-MI and GO-D-MI when the binding affinity of the amino acid for the ion is lower, leading to an increase in fluorescence. At the same time, dopamine could be oxidized by GO-M-MI or GO-D-MI via hole transfer from its valence band, leading to fluorescence quenching in the GO structure. These two pathways for fluorescence quenching and de-quenching are competing

View Article Online
DOI: 10.1039/C9NR00643E

in the GO-AA-MI solution in the presence of dopamine. As a result, a quenching response was mainly observed in GO-M-Cu and GO-D-Cu, which have a high binding affinity for Cu^{2+} ions. In contrast, GO-M-Co has a low binding affinity to Co^{2+} ions, thus the fluorescence de-quenching and quenching processes occurred to the same extent and no net change in its fluorescence intensity was observed. For the turn-on fluorescence response of GO-AA-Au structures to norepinephrine, the mechanism proposed for dopamine would not suffice. We speculate that other pathways could be responsible for the fluorescence increase of GO-AA-Au by norepinephrine, which will be thoroughly investigated through follow-up experiments and computational modeling.

4. Cellular detection of dopamine

The performance of the selected GO-Y-Fe sensor when detecting dopamine at physiological concentrations was examined. As shown in Figure 5a, the fluorescence of GO-Y-Fe was gradually quenched as the concentration of dopamine increased from 6.25 to 100 nM. However, GO-Y-Fe displayed no quenching response to either norepinephrine or epinephrine at nanomolar concentrations. The pH effect on the fluorescence response of GO-Y-Fe to three catecholamine neurotransmitters was investigated. As shown in Figure S9, GO-Y-Fe showed the selective fluorescence response to dopamine at pH 7.4. However, its response selectivity for dopamine became weak at both acidic and basic pH. In addition, the fluorescence of GO-Y-Fe remained almost constant in the presence of ascorbic acid (ASA) and uric acid (UA), known abundant interferences in blood, even at much higher concentration (12.5 μM) than dopamine (Figure 5b). The GO-Y-Fe sensor is therefore able to selectively detect dopamine against other catecholamine neurotransmitters and interferences without the use of antibodies. GO-Y-Fe could detect dopamine concentrations as low as 5.5 nM (Figure 5c); thus the dopamine sensing

View Article Online
DOI: 10.1039/C9NR00643E

performance of GO-Y-Fe was compared with that of other detection methods (Table S4). The GO-Y-Fe sensor appears to be more sensitive for dopamine detection than all other methods except an enzyme-linked immunosorbent assay (ELISA). The ELISA, however, requires a much longer time (480 min) than the GO-Y-Fe sensor (10 min) for dopamine detection due to having multiple procedures. The GO-Y-Fe sensor was also able to differentiate dopamine from the similar structures of norepinephrine and epinephrine without the use of antibodies in a rapid and simple manner. As compared with aptamers-based dopamine sensors,[61-65] it is much simpler and faster to design GO-AA-MI sensors capable of selectively detecting dopamine. Only three synthetic steps can produce a variety of GO-AA-MI sensors. In addition, GO-AA-MI sensors are more cost-effective than aptamers-based sensors. Note that there have been a few reports for aptamer-based sensors that can discriminate dopamine from other catecholamines such as norepinephrine and epinephrine to date.

Finally, the GO-Y-Fe sensor was applied to the detection of dopamine secreted from living cells. The cytotoxicity of the GO-Y-Fe sensor was first explored in rat pheochromocytoma (PC-12) cells using a cell counting kit-8 (CCK-8) assay (Figure 6a-6b). The cell viability remained similar as the concentration of the sensor increased from 10 to 100 μg/mL, indicating that the GO-Y-Fe is biocompatible. In order to detect dopamine secreted from PC-12 cells, the cells were incubated for a certain period of time, and the cell medium was collected at regular time intervals to be added to the GO-Y-Fe sensor solution, followed by measuring the fluorescence intensity of the GO-Y-Fe sensor. As shown in Figure 6c, the fluorescence of the GO-Y-Fe sensor gradually decreased as a function of incubation time (black line), indicating that the dopamine concentration in the cell medium increased. To confirm the concentration of dopamine secreted from the cells, an ELISA was carried out, also showing that dopamine

View Article Online
DOI: 10.1039/C9NR00643E

concentration increased as a function of incubation time (red line). The fluorescence quenching extent of the GO-Y-Fe sensor correlated with the concentration of dopamine secreted from the cells. These results clearly suggest that the GO-Y-Fe sensor was able to detect dopamine in living cells in a rapid, simple, and sensitive manner.

Conclusions

We demonstrated a chemical approach for controlling the selectivity and sensitivity of the GO fluorescence response to neurotransmitters, through organometallic complexation of GO using amino acids and metal ions. The fluorescence response of GO-AA-MI derivatives was effectively modulated by varying the amino acids and metal ions, leading to the creation of the sensors, GO-M-Cu and GO-Y-Fe, which showed a selective fluorescence quenching response to dopamine. The GO-Y-Fe sensor developed was then able to selectively and sensitively detect dopamine against other catecholamine neurotransmitters and interferences without the use of antibodies in a rapid and simple manner. In addition, the sensor could detect dopamine secreted from living neurons. This demonstrated that this chemical approach for the modulation of fluorescence responses to target molecules could be applied to other sensing methods, and this new type of biosensor could be extended to detect diverse biological molecules.

Conflicts of interest

The authors declare no competing financial interests.

Acknowledgements

View Article Online
DOI: 10.1039/C9NR00643E

This work was supported by the Basic Science Research Program (NRF-2014R1A2A1A11051877 and NRF-2017R1A2B2008455) through the National Research Foundation of Korea funded by the Ministry of Science and ICT.

ReferencesUncategorized References

1. P. D. Howes, R. Chandrawati and M. M. Stevens, *Science*, 2014, **346**, 53-+.
2. J. Lee, J. Kim, S. Kim and D. H. Min, *Adv Drug Deliver Rev*, 2016, **105**, 275-287.
3. Z. Farka, T. Juriik, D. Kovaar, L. Trnkova and P. Sklaadal, *Chem Rev*, 2017, **117**, 9973-10042.
4. G. Vlatakis, L. I. Andersson, R. Muller and K. Mosbach, *Nature*, 1993, **361**, 645-647.
5. T. Kajisa and T. Sakata, *Acs Appl Mater Inter*, 2018, **10**, 34983-34990.
6. J. Q. Zhang, M. P. Landry, P. W. Barone, J. H. Kim, S. C. Lin, Z. W. Ulissi, D. H. Lin, B. Mu, A. A. Boghossian, A. J. Hilmer, A. Rwei, A. C. Hinckley, S. Kruss, M. A. Shandell, N. Nair, S. Blake, F. Sen, S. Sen, R. G. Croy, D. Y. Li, K. Yum, J. H. Ahn, H. Jin, D. A. Heller, J. M. Essigmann, D. Blankschtein and M. S. Strano, *Nat Nanotechnol*, 2013, **8**, 959-968.
7. T. W. Kang, J. Han, S. Lee, I. J. Hwang, S. J. Jeon, J. M. Ju, M. J. Kim, J. K. Yang, B. Jun, C. H. Lee, S. U. Lee and J. H. Kim, *Nat Commun*, 2018, **9**.
8. X. K. Ding and K. L. Yang, *Anal Chem*, 2013, **85**, 10710-10716.
9. S. J. Jeon, S. Y. Kwak, D. Yim, J. M. Ju and J. H. Kim, *J Am Chem Soc*, 2014, **136**, 10842-10845.
10. H. J. Wu, Y. J. Li, J. Fan, Z. A. Deng, Z. Hu, X. W. Liu, E. A. Graviss, M. Ferrari, X. Ma and Y. Hu, *Anal Chem*, 2014, **86**, 1988-1996.
11. M. J. Kim, S. J. Jeon, T. W. Kang, J. M. Ju, D. Yim, H. I. Kim, J. H. Park and J. H. Kim, *Acs Appl Mater Inter*, 2017, **9**, 12316-12323.
12. D. Xie, W. F. Zhu, H. Cheng, Z. Y. Yao, M. Li and Y. L. Zhao, *Phys Chem Chem Phys*, 2018, **20**, 8881-8886.
13. H. Q. Shi, W. B. Tsai, M. D. Garrison, S. Ferrari and B. D. Ratner, *Nature*, 1999, **398**, 593-597.
14. K. Haupt and K. Mosbach, *Chem Rev*, 2000, **100**, 2495-2504.
15. J. M. Pan, W. Chen, Y. Ma and G. Q. Pan, *Chem Soc Rev*, 2018, **47**, 5574-5587.
16. W. Q. Zhang, D. W. Duan, S. Q. Liu, Y. S. Zhang, L. P. Leng, X. L. Li, N. Chen and Y. P. Zhang, *Biosens Bioelectron*, 2018, **118**, 129-136.
17. Y. Hoshino, T. Kodama, Y. Okahata and K. J. Shea, *J Am Chem Soc*, 2008, **130**, 15242-+.
18. E. J. Cho, J. W. Lee and A. D. Ellington, *Annu Rev Anal Chem*, 2009, **2**, 241-264.
19. A. D. Ellington and J. W. Szostak, *Nature*, 1990, **346**, 818-822.
20. M. R. Dunn, R. M. Jimenez and J. C. Chaput, *Nat Rev Chem*, 2017, **1**.
21. K. S. Park, *Biosens Bioelectron*, 2018, **102**, 179-188.
22. M. Darvas and R. D. Palmiter, *J Neurosci*, 2010, **30**, 1158-1165.

View Article Online
DOI: 10.1039/C9NR00643E

23. A. Usiello, J. H. Baik, F. Rouge-Pont, R. Picetti, A. Dierich, M. LeMeur, P. V. Piazza and E. Borrelli, *Nature*, 2000, **408**, 199-203.
24. J. Jankovic, *J Neurol Neurosur Ps*, 2008, **79**, 368-376.
25. P. S. Rao, N. Rujikarn, J. M. Luber and D. H. Tyras, *Chromatographia*, 1989, **28**, 307-310.
26. T. Pradhan, H. S. Jung, J. H. Jang, T. W. Kim, C. Kang and J. S. Kim, *Chem Soc Rev*, 2014, **43**, 4684-4713.
27. J. J. Zhao, L. M. Zhao, C. Q. Lan and S. L. Zhao, *Sensor Actuat B-Chem*, 2016, **223**, 246-251.
28. J. L. Chen, X. P. Yan, K. Meng and S. F. Wang, *Anal Chem*, 2011, **83**, 8787-8793.
29. A. Yildirim and M. Bayindir, *Anal Chem*, 2014, **86**, 5508-5512.
30. D. Y. Zhao, G. L. Yu, K. L. Tian and C. X. Xu, *Biosens Bioelectron*, 2016, **82**, 119-126.
31. P. L. dos Santos, V. Katic, K. C. F. Toledo and J. A. Bonacin, *Sensor Actuat B-Chem*, 2018, **255**, 2437-2447.
32. A. F. Khan, D. A. C. Brownson, E. P. Randviir, G. C. Smith and C. E. Banks, *Anal Chem*, 2016, **88**, 9729-9737.
33. D. Wen, W. Liu, A. K. Herrmann, D. Haubold, M. Holzschuh, F. Simon and A. Eychmuller, *Small*, 2016, **12**, 2439-2442.
34. J. Kim, M. Jeon, K. J. Paeng and I. R. Paeng, *Anal Chim Acta*, 2008, **619**, 87-93.
35. K. R. Jiang, Y. N. Wang, G. Thakur, Y. Kotsuchibashi, S. Naicker, R. Narain and T. Thundat, *Acs Appl Mater Inter*, 2017, **9**, 15225-15231.
36. T. Kajisa, W. Li, T. Michinobu and T. Sakata, *Biosens Bioelectron*, 2018, **117**, 810-817.
37. W. S. Hummers and R. E. Offeman, *J Am Chem Soc*, 1958, **80**, 1339-1339.
38. T. Gokus, R. R. Nair, A. Bonetti, M. Bohmler, A. Lombardo, K. S. Novoselov, A. K. Geim, A. C. Ferrari and A. Hartschuh, *Acs Nano*, 2009, **3**, 3963-3968.
39. K. P. Loh, Q. L. Bao, G. Eda and M. Chhowalla, *Nat Chem*, 2010, **2**, 1015-1024.
40. Z. T. Luo, P. M. Vora, E. J. Mele, A. T. C. Johnson and J. M. Kikkawa, *Appl Phys Lett*, 2009, **94**.
41. Q. S. Mei, K. Zhang, G. J. Guan, B. H. Liu, S. H. Wang and Z. P. Zhang, *Chem Commun*, 2010, **46**, 7319-7321.
42. G. Eda, Y. Y. Lin, C. Mattevi, H. Yamaguchi, H. A. Chen, I. S. Chen, C. W. Chen and M. Chhowalla, *Adv Mater*, 2010, **22**, 505-+.
43. C. Galande, A. D. Mohite, A. V. Naumov, W. Gao, L. J. Ci, A. Ajayan, H. Gao, A. Srivastava, R. B. Weisman and P. M. Ajayan, *Sci Rep-Uk*, 2011, **1**.
44. E. Morales-Narvaez and A. Merkoci, *Adv Mater*, 2012, **24**, 3298-3308.
45. C. Chung, Y. K. Kim, D. Shin, S. R. Ryoo, B. H. Hong and D. H. Min, *Accounts Chem Res*, 2013, **46**, 2211-2224.
46. V. Georgakilas, J. N. Tiwari, K. C. Kemp, J. A. Perman, A. B. Bourlinos, K. S. Kim and R. Zboril, *Chem Rev*, 2016, **116**, 5464-5519.
47. L. Wang, X. Xin, M. Z. Yang, X. Ma, Z. Y. Feng, R. Chen, J. L. Shen and S. L. Yuan, *Phys Chem Chem Phys*, 2014, **16**, 20932-20940.
48. J. L. Shen, X. Xin, Y. J. Zhang, L. F. Song, L. Wang, W. Y. Tang and Y. J. Ren, *Carbohyd Polym*, 2015, **117**, 592-599.
49. R. R. Xue, X. Xin, L. Wang, J. L. Shen, F. R. Ji, W. Z. Li, C. Y. Jia and G. Y. Xu, *Phys Chem Chem Phys*, 2015, **17**, 5431-5440.

View Article Online
DOI: 10.1039/C9NR00643E

50. J. L. Shen, X. Xin, T. Liu, L. Tong, G. Y. Xu and S. L. Yuan, *J Colloid Interf Sci*, 2016, **468**, 78-85.
51. M. Roy, T. S. Kusurkar, S. K. Maurya, S. K. Meena, S. K. Singh, N. Sethy, K. Bhargava, R. K. Sharma, D. Goswami, S. Sarkar and M. Das, *3 Biotech*, 2014, **4**, 67-75.
52. J. H. Jung, D. S. Cheon, F. Liu, K. B. Lee and T. S. Seo, *Angew Chem Int Edit*, 2010, **49**, 5708-5711.
53. T. W. Kang, S. J. Jeon, H. I. Kim, J. H. Park, D. Yim, H. R. Lee, J. M. Ju, M. J. Kim and J. H. Kim, *Acs Nano*, 2016, **10**, 5346-5353.
54. S. Y. Kwak, J. K. Yang, S. J. Jeon, H. I. Kim, J. Yim, H. Kang, S. Kyeong, Y. S. Lee and J. H. Kim, *Adv Funct Mater*, 2014, **24**, 5119-5128.
55. J. K. Yang, S. Y. Kwak, S. J. Jeon, E. Lee, J. M. Ju, H. I. Kim, Y. S. Lee and J. H. Kim, *Nanoscale*, 2016, **8**, 12272-12281.
56. A. Mishra and M. Soni, *Metal-based drugs*, 2008, **2008**.
57. B. B. Mahapatra, B. Patel, D. Satyanarayana and S. K. Pujari, *Acta Chim Hung*, 1983, **114**, 217-221.
58. J. M. Costa-Fernandez, R. Pereiro and A. Sanz-Medel, *Trac-Trend Anal Chem*, 2006, **25**, 207-218.
59. J. Jover, R. Bosque and J. Sales, *Dalton T*, 2008, DOI: 10.1039/b805860a, 6441-6453.
60. J. Balla, T. Kiss and R. F. Jameson, *Inorg Chem*, 1992, **31**, 58-62.
61. E. Farjami, R. Campos, J. S. Nielsen, K. V. Gothelf, J. Kjems and E. E. Ferapontova, *Anal Chem*, 2013, **85**, 121-128.
62. J. Y. Xu, Y. Li, L. K. Wang, Y. J. Huang, D. L. Liu, R. Sun, J. L. Luo and C. Y. Sun, *Dyes Pigments*, 2015, **123**, 55-63.
63. S. Banerjee, Y. J. Hsieh, C. R. Liu, N. H. Yeh, H. H. Hung, Y. S. Lai, A. C. Chou, Y. T. Chen and C. Y. Pan, *Small*, 2016, **12**, 5524-5529.
64. W. J. Hu, Y. Y. Huang, C. Y. Chen, Y. K. Liu, T. A. Guo and B. O. Guan, *Sensor Actuat B-Chem*, 2018, **264**, 440-447.
65. N. Nakatsuka, K. A. Yang, J. M. Abendroth, K. M. Cheung, X. B. Xu, H. Y. Yang, C. Z. Zhao, B. W. Zhu, Y. S. Rim, Y. Yang, P. S. Weiss, M. N. Stojanovic and A. M. Andrews, *Science*, 2018, **362**, 319-+.

View Article Online
DOI: 10.1039/C9NR00643E

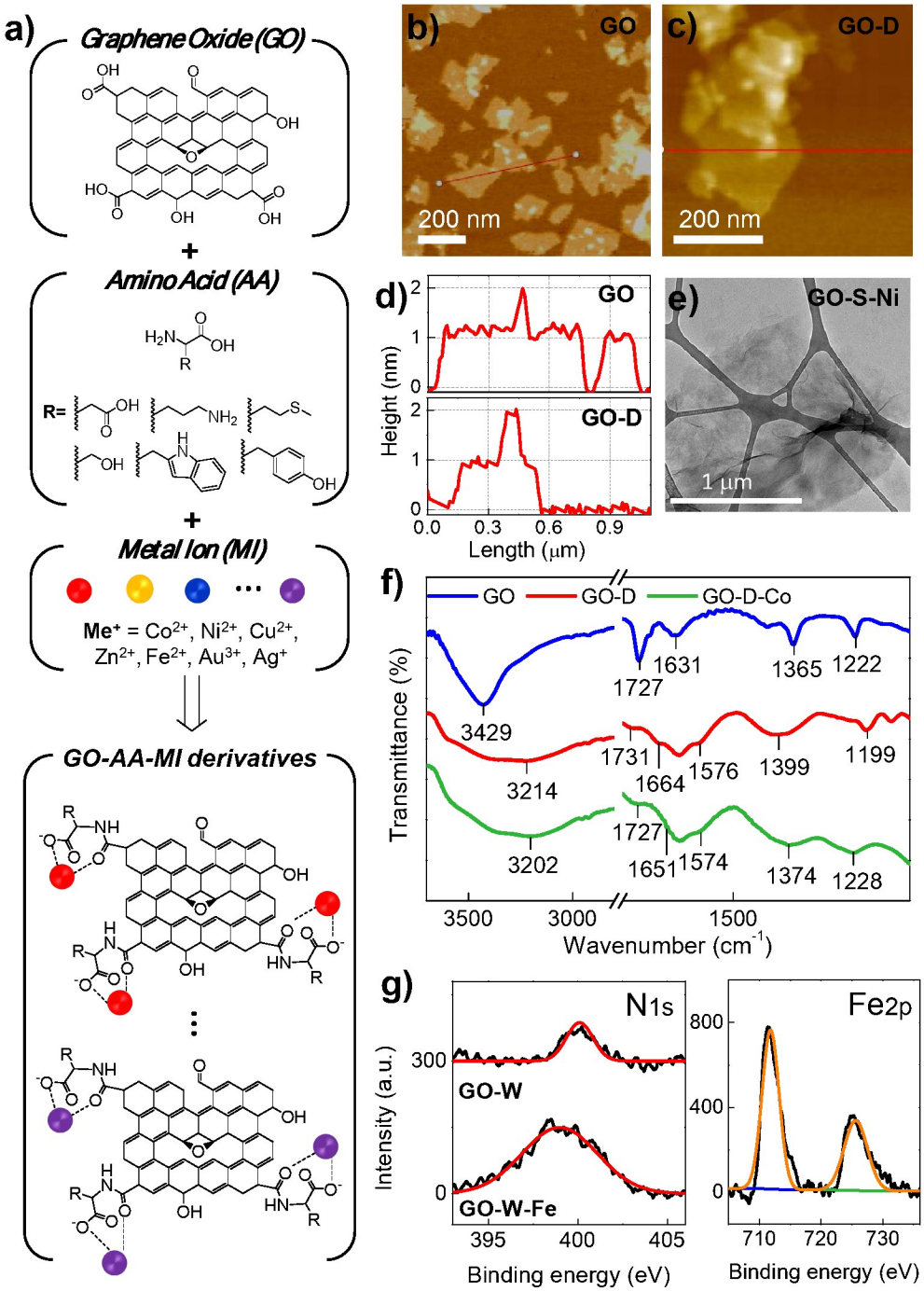

Figure 1. Characterization of GO-AA-MI derivatives. (a) Schematic illustration for the construction of GO-AA-MI derivatives. AFM image of (b) GO and (c) GO-D, and (d) their height profiles along the red line on the AFM images. (e) TEM image of GO-S-Ni. (f) FT-IR spectra of GO, GO-D, and GO-D-Co. (g) N1s and Fe2p XPS spectra of GO-W-Fe.

View Article Online
DOI: 10.1039/C9NR00643E

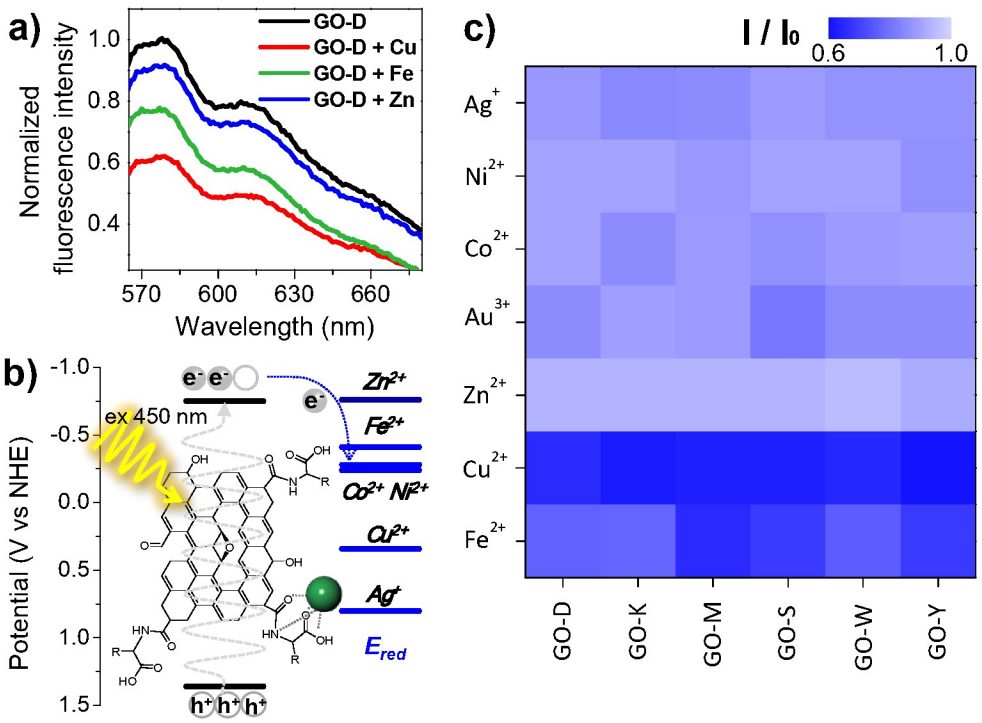

Figure 2. Fluorescence response of five GO-AA structures to metal ions. (a) Fluorescence spectra of GO-D in the absence and the presence of Zn^{2+}, Cu^{2+}, and Fe^{2+} ions. (b) Energy diagram for electron transfer from GO-AA to metal ions. (c) Fluorescence quenching profile of five GO-AA structures for seven metal ions at 25 μM. I and I_o indicate the fluorescence intensity with and without metal ions, respectively, under 450 nm excitation.

View Article Online
DOI: 10.1039/C9NR00643E

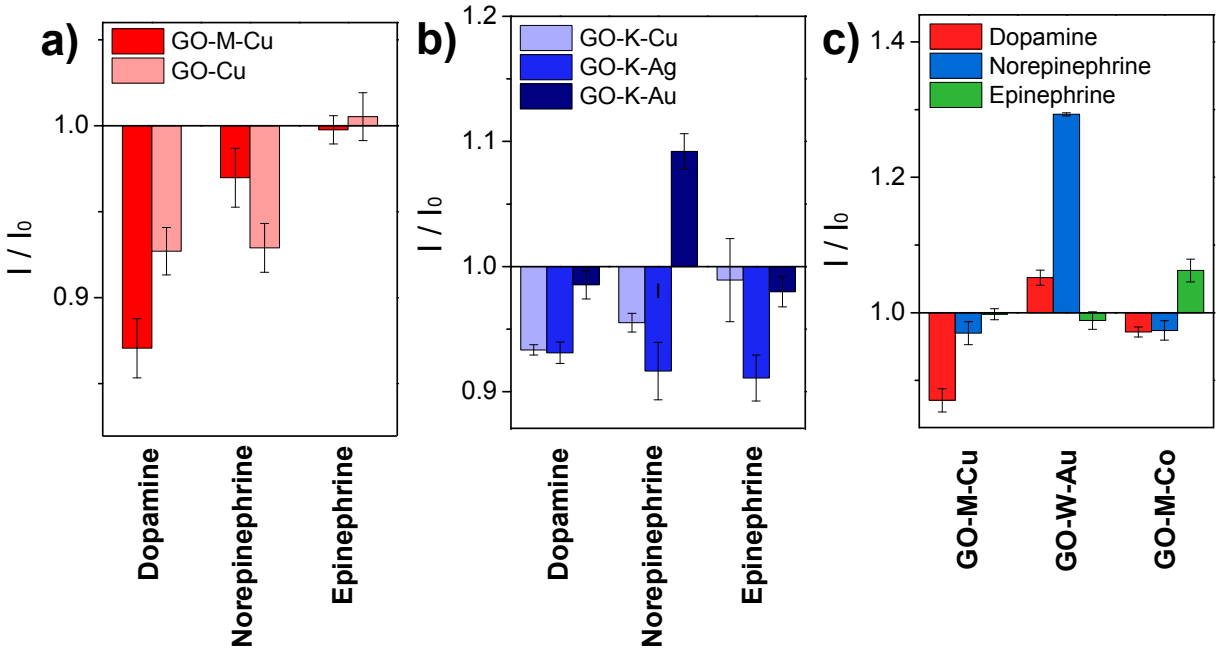

Figure 3. Effects of amino acids and metal ions on the fluorescence response of GO-AA-MI derivatives to neurotransmitters. (a) Fluorescence response of GO-Cu and GO-M-Co to dopamine, norepinephrine, and epinephrine at 6.25 μM. (b) Fluorescence response of GO-K-Cu, GO-K-Ag, and GO-K-Au to the three neurotransmitters. (c) Fluorescence response of GO-AM-Cu, GO-W-Au, and GO-M-Co to dopamine, norepinephrine, and epinephrine. I and I_o indicate the fluorescence intensity with and without addition of each neurotransmitter, respectively, under 450 nm excitation.

View Article Online
DOI: 10.1039/C9NR00643E

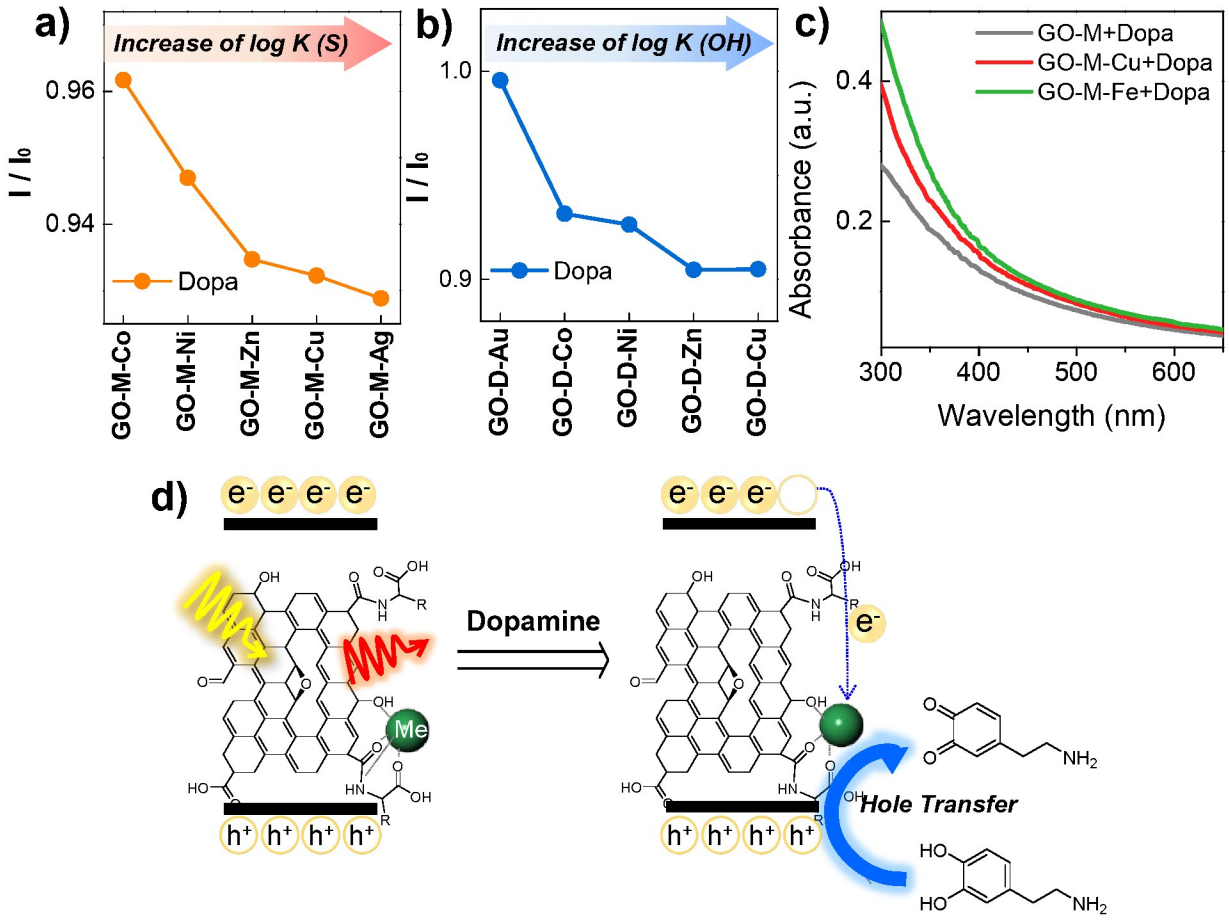

Figure 4. Proposed mechanism responsible for the fluorescence response of GO-AA-MI derivatives to dopamine. (a) Plot of the fluorescence response of GO-M-MI structures to dopamine versus the binding affinity of the sulfide of methionine to metal ions. (b) Plot of the fluorescence response of GO-D-MI structures to dopamine versus the binding affinity of the hydroxyl group of aspartic acid to metal ions. (c) Absorption spectra of GO-M, GO-M-Cu, and GO-M-Fe taken 5 min after the addition of dopamine at 6.25 μM. (d) Mechanism of the fluorescence quenching of GO-AA-MI derivatives by dopamine. I and I_o indicate the fluorescence intensity with and without addition of dopamine, respectively, under 450 nm excitation.

View Article Online
DOI: 10.1039/C9NR00643E

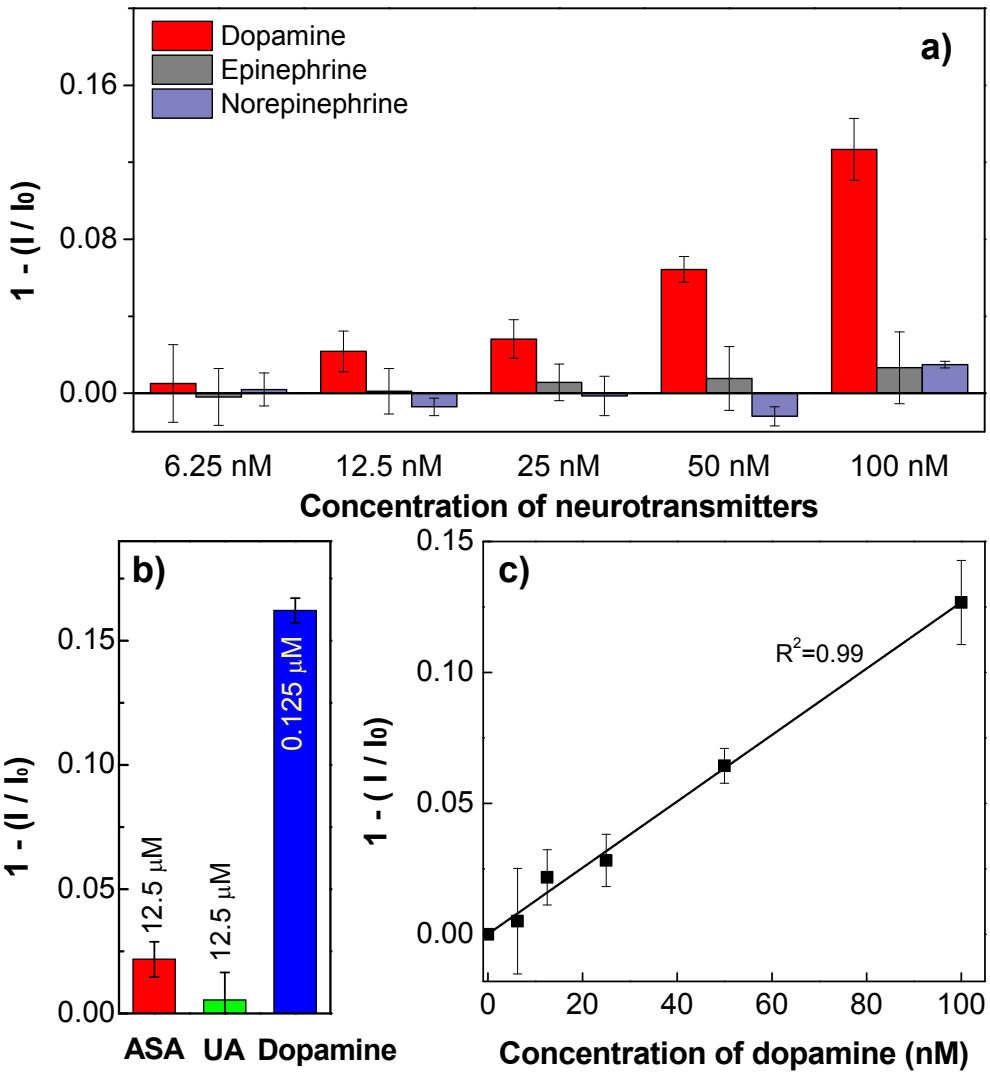

Figure 5. Selectivity and sensitivity of GO-Y-Fe for dopamine detection. (a) Fluorescence response of GO-Y-Fe to dopamine, epinephrine, and norepinephrine at nanomolar concentrations. (b) Fluorescence response of GO-Y-Fe to ascorbic acid (ASA) and uric acid (UA). (c) Calibration curve of GO-Y-Fe as a function of dopamine concentration. I and I_o indicate the fluorescence intensity with and without addition of each neurotransmitter, respectively, under 450 nm excitation.

View Article Online
DOI: 10.1039/C9NR00643E

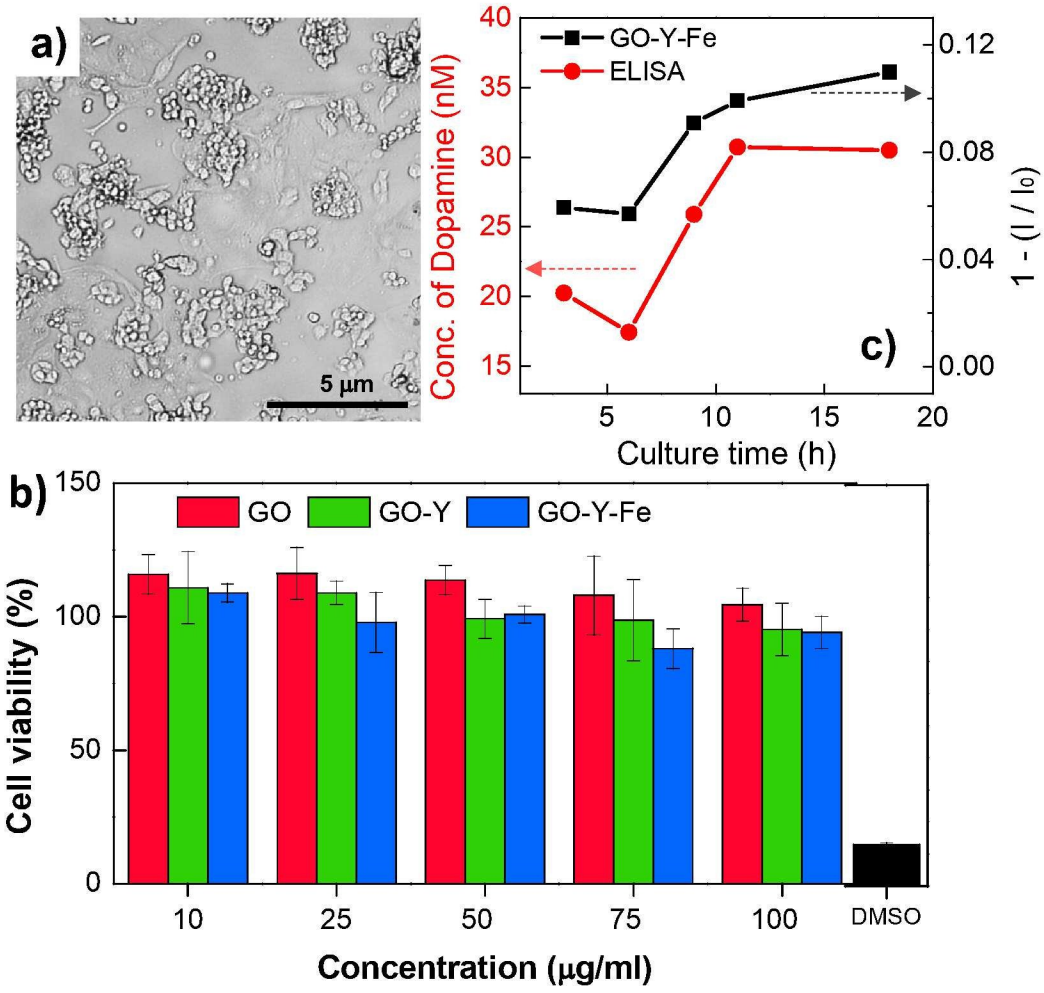

Figure 6. Cellular detection of dopamine over GO-Y-Fe. (a) Optical image of PC-12 cells. (b) Cytotoxicity of GO, GO-Y, and GO-Y-Fe in PC-12 cells using a CCK-8 assay. (c) Fluorescence response of GO-Y-Fe to dopamine in the cell medium, and quantification of the dopamine concentration using ELISA. I and I_o indicate the fluorescence intensity with and without addition of the cell medium, respectively, under 450 nm excitation.

View Article Online
DOI: 10.1039/C9NR00643E

TOC

Graphene oxide fluorescence is modulated by organometallic complexes for the antibody-free and selective detection of dopamine.